Synthesis by the polyol process and ionic conductivity of nanostructured La2Mo2O9 powders

H. Sellemi, Sandrine Coste, Maud Barré, R. Retoux, A. Ben Ali, P. Lacorre

Synthesis by the polyol process and ionic conductivity of nanostructurated $La_2Mo_2O_9$ powders

H. Sellemi[a,b], S. Coste[a*], M. Barre[a], R. Retoux[c], A. Ben Ali[b], P. Lacorre [a]

[a] LUNAM Université, Université du Maine, UMR CNRS 6283, Institut des Molécules et Matériaux du Mans (IMMM), département Oxydes et Fluorures, Avenue Olivier Messiaen, 72085 Le Mans Cedex, France

[b] University of Carthage, Faculté des Sciences de Bizerte, Unité de Recherche Synthèse et structure de nanomatériaux UR11ES30, 7021 Jarzouna, Tunisie

[c] Laboratoire CRISMAT UMR CNRS 6508, ENSICAEN, 6 boulevard Maréchal Juin, 14050 Caen Cedex, France

e-mails :

Houssem Sellemi : sellemi.houssem@gmail.com

Sandrine Coste : sandrine.coste@univ-lemans.fr

Maud Barre : maud.barre@univ-lemans.fr

Richard Retoux : richard.retoux@ensicaen.fr

Amor Ben Ali : Amor.BenAli@fsb.rnu.tn

Philippe Lacorre : philippe.lacorre@univ-lemans.fr

Corresponding author :

Sandrine Coste : sandrine.coste@univ-lemans.fr

Abstract

$La_2Mo_2O_9$ nanostructured powders were synthesized by the polyol process. The effects of the nature of the polyol, the refluxing time, the hydrolysis ratio, the metal concentration and the addition of hydroxyde ions, on the purity and morphology of the powders are determined. Two main morphologies are observed, the particles being in the shape of platelets or spheres, with respectively diethylene glycol or ethylene glycol as solvent. A specific surface area of 24 $m^2.g^{-1}$ was reached by varying the metal concentration. The conductivity measurements were recorded on pellets that present in some cases a closed porosity, the relative density reaching 95% without any milling step. According to the synthesis parameters, the grain conductivity can be slightly increased, the total conductivity remaining only slightly lower than that of pellets made of powders synthesized by solid state reaction.

Keywords

Nanostructured materials, $La_2Mo_2O_9$, polyol process, ionic conductivity

1. Introduction

Recently, $La_2Mo_2O_9$-based oxide-ion conductors have attracted special attention as they present high ionic conductivity at low temperatures (400–800 °C) under a wide oxygen partial pressure ranging from 0.21 to 10^{-15} atm [1–5]. Pure $La_2Mo_2O_9$ presents a phase transition from a monoclinic low temperature α-form to a cubic high temperature β-form at about 580 °C [1,2]. At this temperature, the ionic conductivity of $La_2Mo_2O_9$ increases by two orders of magnitude and, above it becomes higher than that of yttria-stabilized zirconia (YSZ), which is the reference material among solid electrolytes for oxygen ion conductors. $La_2Mo_2O_9$ is usually prepared by a conventional solid state reaction method [1–6], but this method does not allow to obtain directly dense ceramic samples, since a milling step is necessary before sintering. Indeed, even if this step leads to the decrease of the grain size and thus to a higher sinterability, it also leads to the apparition of impurities, especially when the milling balls/jar are made of zirconia [7, 8]. These impurities are located in the grain boundaries after sintering and increase their resistance, leading to a drop of the total conductivity of the material. Therefore, in order to obtain a good $La_2Mo_2O_9$ conductor, we should synthesize a pure sample with high density. Nanocrystalline powders allow a good densification (when non aggregated), lower sintering temperatures, better mechanical properties of the electrolytes, and generally improve the electrical properties [9]. Recently, we successfully synthesized nanocrystalline $La_2Mo_2O_9$ powders by the polyol process [10], that presents the advantage of inducing various microstructures [11-13] and lowering the temperature of the heat treatment (generally necessary as a final step when soft chemistry is used, in order to reduce the size of the particles obtained [14]).

The first aim of this work was to optimize the synthesis parameters in order to extend the control of the morphology. The following parameters were modified in order to determine their effect on the structure and microstructure of the final powders: the refluxing time, the nature of polyol, the hydrolysis ratio (h), defined by the nominal molar ratio water/total divalent and trivalent metal ions, the metal concentration and the effect of addition of hydroxide ions. The second part of this work was devoted to the measurement of ionic conductivities and the determination of the impact of the morphology, by way of the synthesis process, on them. This part also included, at first, a study of the sinterability of the powders.

2. Experimental

2.1. Synthesis

Precursor salts, lanthanum acetate, $La(CH_3CO_2)_3.1.5\ H_2O$ (Alfa Aesar, 99,99%), and ammonium molybdate, $(NH_4)_2Mo_2O_7$ (Alfa Aesar, Mo 56.5%), in a molar ratio (Mo:La: = 1:1), and, for a part of this work an appropriate volume of distilled water, were added to 30 mL of a given polyol (table

1). The total lanthanum and molybdenum concentration ([La+Mo]) was 0.2 mol.L^{-1}, except for the part concerning the effect of the concentration in which the total concentration was varied from 0.05 to 0.5 mol.L^{-1}. The resulting mixture was then heated up to the boiling point of the polyol, under reflux and mechanical stirring, for durations ranging from 1 to 3 hours. In order to modify the pH and thus try to modify the morphology or the purity of the obtained powders, urea (Jeulin, 99%) was added to the reaction mixture just before heating, for some syntheses. After cooling, the as-prepared precipitates were separated from the supernatant by alternating centrifugation, washing in ethanol and ultrasonication. Finally, the precipitates were heat treated by placing them directly, for 5 min, in a muffle furnace preheated at 600°C and then quenched at room temperature. The aim of such a rapid heat treatment was to avoid an important grain growth. It's worth noting that a slightly higher temperature (600°C instead of 550°C) was used for this work, compared to that in our previous publication [10], in order to facilitate the observation of an eventual impurity.

Table 1 : Nature of the different polyols and reflux temperatures.

Solvent	**Purity (%)**	**Theoretical T_{bp}(°C)**	**T reflux (experimental boiling point)**
Ethyleneglycol (EG)	99.9%, Alfa Aesar	197	192
1,2-Propanediol (PEG)	97%, Acros organics	188	182
Diethyleneglycol (DEG)	99.9%, Aldrich	245	227
Tetraethyleneglycol (TEG)	99.5%, Acros organics	327	312

2.2. Characterization techniques

The phase purity of the obtained powders was checked by recording X-Ray powder Diffraction (XRD) patterns at room temperature on a PANalytical θ/θ Bragg–Brentano X'pert MPD PRO diffractometer ($CuK\alpha_{1+2}$ radiations) equipped with the X'Celerator detector. The diagrams were collected at room temperature in the [10–60°] scattering angle range, with a 0.01671° step for a total acquisition time of 11 min for the presented diagrams, and for a total acquisition time of 1h for the measurement of the full width at half maximum (FWHM) in order to determine the grain size according to the Scherrer equation. For clarity, only selected ranges of these diagrams are presented.

The morphology of the powders was investigated with a Carl Zeiss Supra 55 (Oberkochen, Germany) high resolution scanning electron microscope (SEM) equipped with EDS. The transmission electron microscopy (TEM) study was performed using a 200kV JEOL 2100 LaB_6 transmission electron microscope fitted with a double tilt sample holders. Specimens for TEM observations were prepared by crushing powdered samples in ethanol. After dispersion of the crystallites, a drop of the suspension is deposited and dried onto a carbon coated copper grid. The specific surface area measurements were realized according to the BET method with a Micromeritics Tristar II apparatus. The sinterability of the obtained powders was determined from pellets obtained by pressing the powders unidirectionally under 5000 bars with a 5 mm diameter die, the thickness obtained being of about 2-2.5mm. Nonisothermal sintering behavior of the green pellets was measured on a dilatometer (Model: Netzsch, DIL 402C) from room temperature to 950 °C at a heating rate of 10 °C/min, followed by a cooling down at the same rate.

The electric conductivity was measured by complex impedance spectroscopy on pellets sintered by placing the green pellets directly, for 30 min, in a preheated muffle furnace and then quenching them down to room temperature [15]. Such a heat treatment was called “rapid” and used in order to keep as much as possible the nonostructuration of the grains. Two probe electrical conductivity measurements were carried out using a Solartron 1260 frequency response analyser connected to a Solartron 1296 dielectric interface over the 10MHz–0.01Hz range (ac voltage of 175 mV, 40 points/decade from 10MHz to 1Hz and few points under 1Hz). Complex impedance diagrams were recorded under dry air flow every 25 °C, after a thermal equilibration of 35 min and over the temperature range 302–700°C. Impedance diagrams plotted in the Nyquist complex plane were least squares fitted, using the Z-view 2.8d software, with one or a series combination of two R//CPE elements, assigned to the bulk and -when two elements are used- to the grain boundaries contributions [16].

3. Results and discussion

3.1. Control of the microstructure of the particles

3.1.1. Effect of the refluxing time

In order to determine the effect of the refluxing time, t, reflux was maintained for 1, 2 or 3 hours, the DEG being used as solvent. After heat treatment of the precipitate, pure $La_2Mo_2O_9$ was obtained with a reflux time of 3 hours. However, impurity ($La_2Mo_3O_{12}$) was observed, by XRD, for shorter reflux times (figure. 1). The shorter the reflux time was, the larger the amount of impurity. Afterwards, the reflux time was thus fixed to 3 hours.

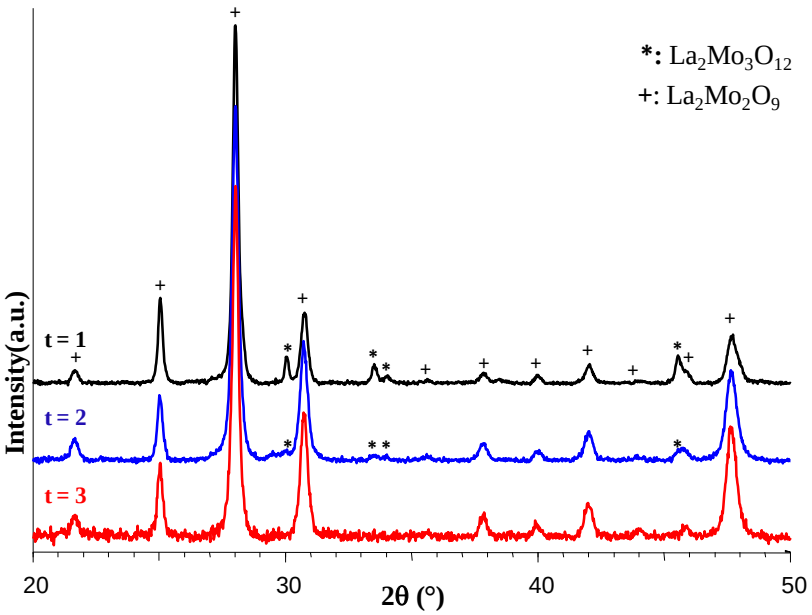

Figure 1: XRD diagrams of precipitates synthesized with DEG with a reflux time of 1, 2 or 3 hours and heat treated at 600°C for 5 min.

3.1.2. Effect of the nature of the polyol

As the nature of the polyol solvent can have a major influence on the particle morphology [11], different polyols were used in order to determine their effects on the microstructure and grain size. Pure $La_2Mo_2O_9$ powders were obtained with DEG whereas $La_2Mo_3O_{12}$ impurity is observed by XRD when EG, PEG and TEG were used as solvent (figure 2). It can be noted that the amount of $La_2Mo_3O_{12}$ impurity is higher with TEG.

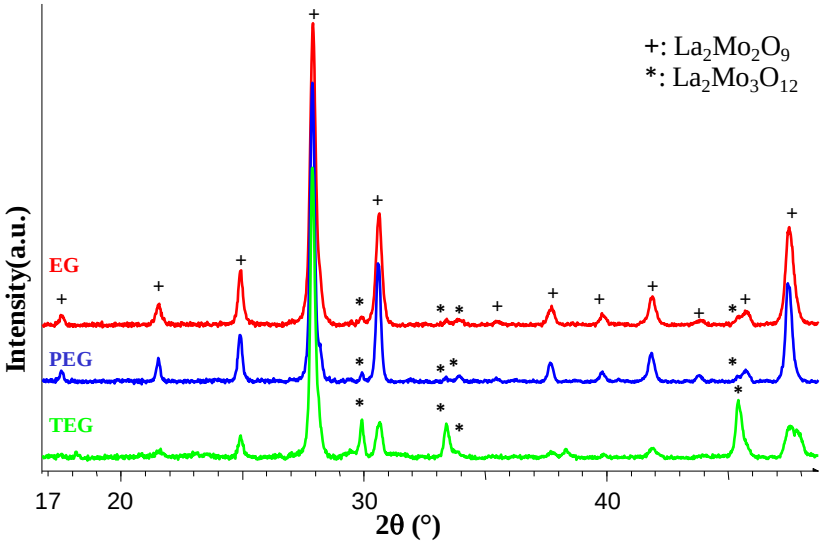

Figure 2: XRD diagrams of precipitates synthesized with different polyols : EG, PEG and TEG and heat treated at 600°C for 5 min.

In order to avoid the formation of the impurity, urea was added to the initial solution (before reflux) in order to promote the precipitation of the lanthanum acetate, as hydroxide or oxide, since the

impurity, $La_2Mo_3O_{12}$, presents a lack of lanthanum. Urea was also added to synthesis with DEG, even if pure $La_2Mo_2O_9$ powders were obtained, in order to determine if its addition can have an impact on the morphology of the powders.

The addition of urea, to the synthesis realized with DEG and EG as solvent, was performed according to the ratios *u* (*u* = [urea]/[La+Mo]) presented in table 2. All the powders obtained with DEG as solvent, after heat treatment, are identified to be pure $La_2Mo_2O_9$ (figure 3 a). In the case of EG as solvent, pure $La_2Mo_2O_9$ is obtained with *u* = 3 whereas $La_2Mo_3O_{12}$ and La_2MoO_6 impurities are observed by XRD for *u* = 2 and *u* = 4 respectively (figure 3 b). These results seem to confirm that the addition of urea, and thus the progressive production of hydroxide groups, enhanced the precipitation of the lanthanum acetate. On another hand, an important release of hydroxide groups seems to stabilize the ammonium molybdate and thus leads to a decrease of its precipitation, leading to the formation of an impurity poor in molybdenum, La_2MoO_6.

Table 2: Ratios of urea, *u*, added to the starting solution and characterization of the powders.

solvent	[urea]/[La+Mo]	impurity	Size(nm)	S_{BET} ($m^2.g^{-1}$)
DEG	1	none	29	15
DEG	2	none	43	9
DEG	3	none	35	11
EG	2	La_2MoO_6	---	
EG	3	none	50	6
EG	4	$La_2Mo_3O_{12}$	---	
PEG	3	none	46	10
TEG	3	none	52	4

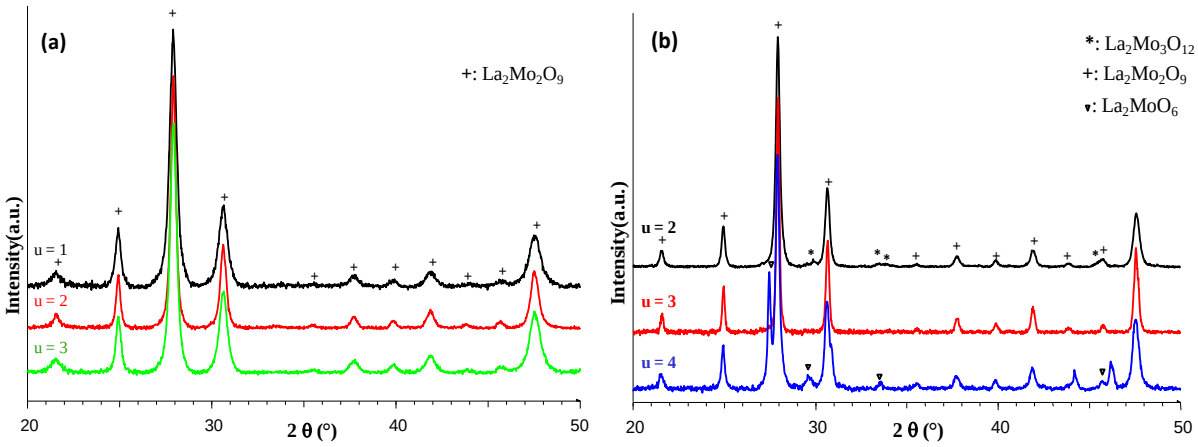

Figure 3: XRD diagrams of precipitates synthesized a) with DEG (*u* = 1, 2 or 3) and b) with EG (*u* = 2, 3 or 4) and heat treated at 600°C for 5 min.

In order to also obtain pure $La_2Mo_2O_9$ powders with PEG and TEG as solvent, the addition of urea was tested with a ratio *u* = 3 as it leads to pure powders with EG as solvent (table 2). With

these 2 polyols, the powders obtained after heat treatment were also pure, as determined by XRD (figure 4).

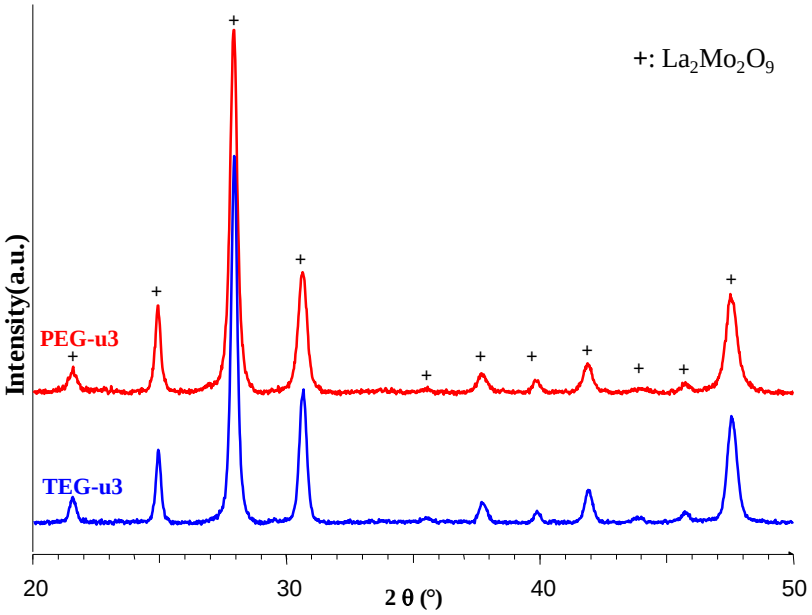

Figure 4: XRD diagrams of precipitates synthesized with PEG (u = 3) or TEG (u = 3) and heat treated at 600°C for 5min.

It can be thus expected that, except in the case of the use of DEG as solvent which leads to pure powders with or without the addition of urea, it is necessary to provide hydroxide groups, through the decomposition of urea during heating of the starting solution, to enhance the precipitation of lanthanum acetate. However, the ratio of urea, u, has to be controlled since a too important value of u leads to a lack of the precipitation of the ammonium molybdate.

The microstructure of the pure $La_2Mo_2O_9$ powders obtained with the different polyols was investigated in order to determine if the nature of the polyol and, for DEG, if the addition of urea impact the morphology of the obtained powders.

The crystallite size was estimated, from XRD patterns, according to the Scherrer equation (the contribution of the apparatus on the FWHM being deducted). From the thinnest diffraction peak at about 2θ =24.9° when we use DEG, the crystallite size is around 29, 43 and 35 nm for u = 1, u = 2 and u = 3 respectively. With EG and u = 3, the crystallite size is about 50 nm.

In order to determine the microstructure of the powders obtained and to estimate if the crystallite size determined by XRD corresponds to monocristallized grains or to particles composed of different crystalline domains, the powders have been observed by SEM (figure 5). After a rapid heat treatment of 5 min at 600°C, the powder synthesized with DEG is composed of platelets of few hundred nanometers long and around twenty nanometers thick. It can also be observed that the addition of urea has no effect on the morphology of samples synthesized in DEG (figure 5.a) but the powder synthesis in EG is composed of almost spherical particles (figure 5.b).

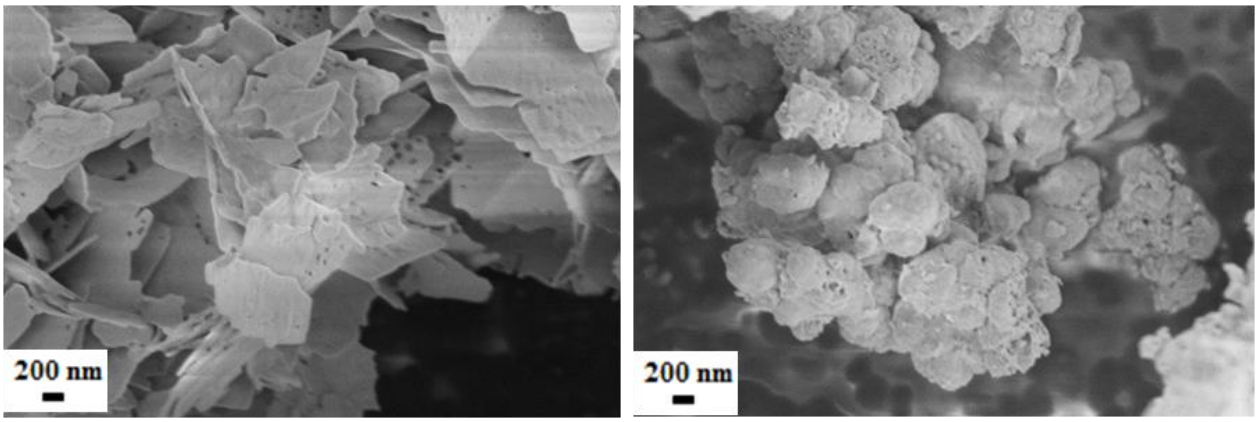

Figure 5: SEM images of precipitates synthesized with DEG (u = 3) (a) or with EG (u = 3) (b) and heat treated at 600°C for 5min.

A TEM micrograph of a sample prepared with EG (u = 3) and heat treated at 600°C for 5min, is given in figure 6. It shows that all the particles are roughly spherical, mostly agglomerated.

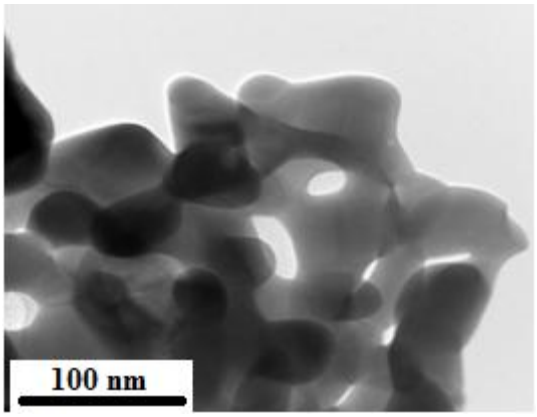

Figure 6: TEM images of the precipitate synthesized with EG (u=3) and heat treated at 600°C for 5min.

SEM observations (figure 7) evidence a difference in morphology between syntheses with TEG and EG as solvent and syntheses with PEG. With EG and TEG, agglomerated spherical particles are observed, but with PEG porous desert-rose like agglomerates are formed.

PEG

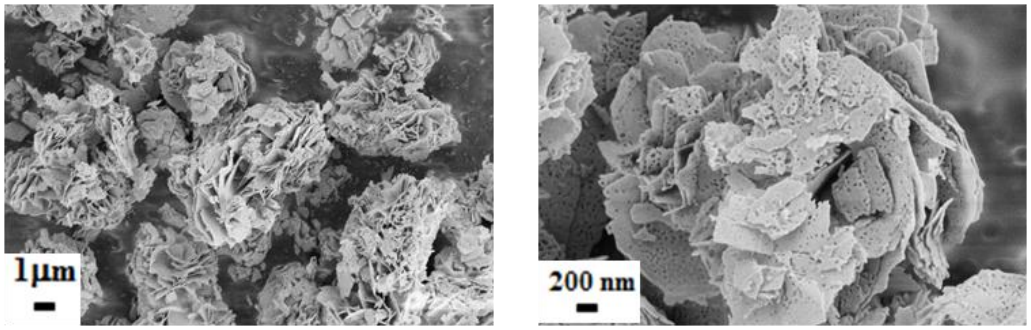

TEG

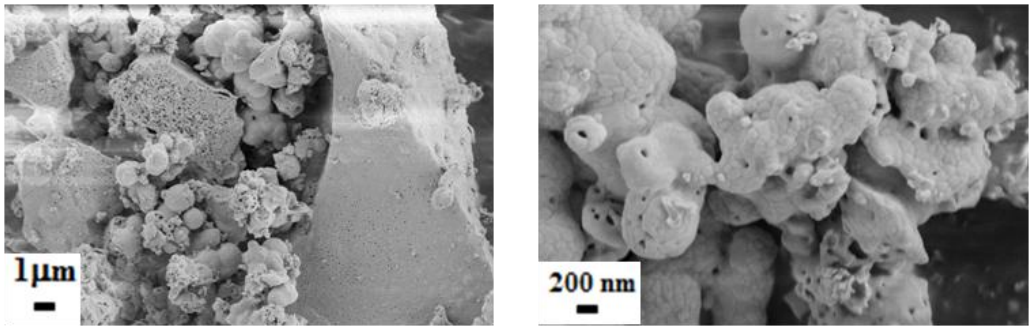

Figure 7: SEM images of precipitates synthesized with PEG (u = 3) or TEG (u = 3) and heat treated at 600°C for 5min.

We measured the specific surface area, according to the BET method, of the powders obtained with all polyols after rapid heat treatment at 600 °C for 5min, these compounds being pure according to XRD. The specific surface area depends on the morphology of the powders. For particles as platelets, the specific surface area is of 16 and 10 $m^2.g^{-1}$ respectively for powders synthesized with DEG (u = 0) or PEG (u = 3) as solvent, which is higher than the surface areas of spherical particles synthesized with EG or TEG as solvent with addition of urea (u = 3) (6 and 4 $m^2.g^{-1}$ respectively) (table 2). These low values result from the agglomeration of the formed particles, especially in the case of spherical ones. The platelets are formed of a plurality of crystallites, but this configuration, in the form of plates, keeps a much larger contact surface.

The contribution of the hydroxide ion seems to lead to a slight decrease in surface area. This slight decrease may be related to an organization of platelets as desert roses during the addition of urea. For comparison, the specific surface areas presented by Kuang *et al.* [17] for $La_2Mo_2O_9$ powders obtained from citrates reaches 4.8 $m^2.g^{-1}$ with a heat treatment at 650°C for 4h.

3.1.3. Effect of the hydrolysis ratio h

Here we studied the effect of the hydrolysis ratio h by adding an appropriate amount of distilled water in DEG (u = 0) or EG (u = 3) with a concentration of metal [La^{3+} + Mo^{6+}] of 0.2 $mol.L^{-1}$. The hydrolysis ratio was varied between 2 and 50 (table 3). The duration of heating under reflux was 3h and the precipitates were heat treated for 5 min at 600 °C.

Table 3: Hydrolysis ratio *h*, added to the starting solution and characterization of the powders.

Solvent	**hydrolysis ratio *h***	**T reflux (experimental boiling point)**	**Size(nm)**	**S_{BET} ($m^2.g^{-1}$)**
DEG	0	227	41	16
DEG	2	220	56	8
DEG	10	203	---	---
DEG	20	193	---	---
DEG	50	172	---	---
EG	0	192	50	6
EG	2	189	52	4
EG	10	179	57	1
EG	20	168	---	---
EG	50	154	---	---

When DEG is used as solvent, the formation of pure $La_2Mo_2O_9$ after a heat treatment at 600 °C for 5 min is observed only with $h \leq 2$, the samples with higher values of h (h >2) containing the $La_2Mo_3O_{12}$ as impurity (figure 8). With EG, $La_2Mo_2O_9$ compound is pure after a heat treatment at 600 °C for 5 min with only $h \leq 10$ (figure 9), according to XRD diagrams. The increase in hydrolysis rate leads, on the other hand, to an increase of crystallite size.

The addition of water seems to promote the precipitation of molybdenum and / or the stabilization of lanthanum acetate, an impurity rich in molybdenum ($La_2Mo_3O_{12}$) being formed. It is possible that the decrease in boiling point due to the presence of water can explain the formation of this impurity. Indeed, we tried to promote germination at lower temperature by performing a first step at 150 °C for 3 h before increasing the temperature to the boiling point, but we observed the formation of the same impurity ($La_2Mo_3O_{12}$). The presence of water may also makes the environment less reducing as the supernatant is colorless after reflux and the precipitate white, whereas they are brown and beige respectively in all the other cases.

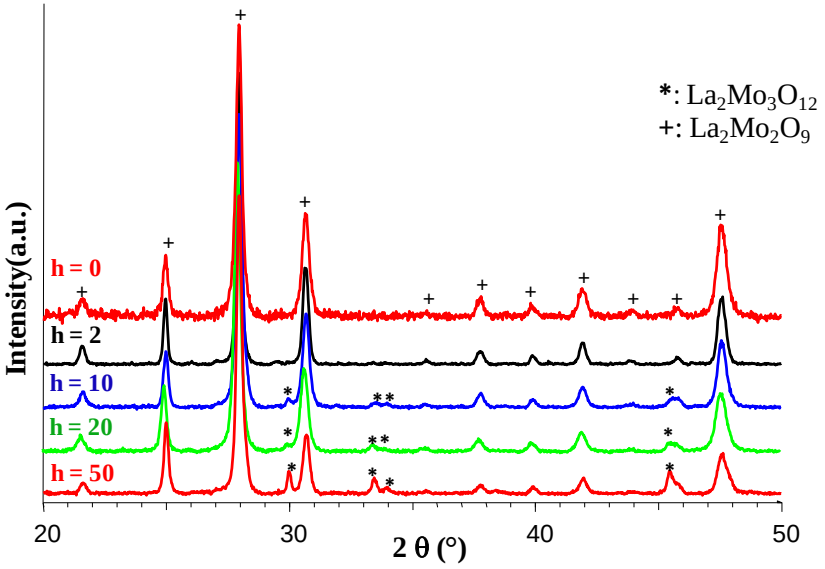

Figure 8: XRD diagrams of the precipitate synthesized with DEG and hydrolysis ratio *h* equal 0, 2, 10, 20 and 50 and heat treated at 600°C for 5min

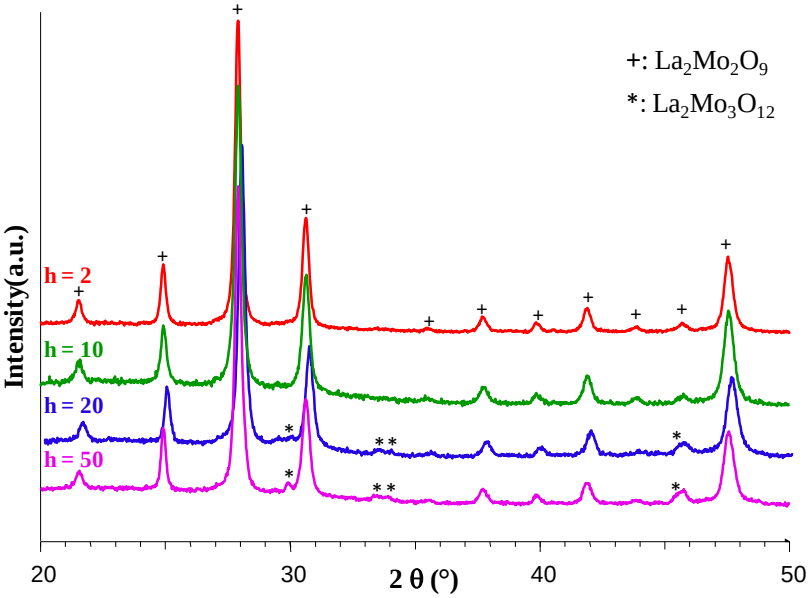

Figure 9: XRD diagrams of the precipitate synthesized with EG and hydrolysis ratio *h* equal 0, 2, 10, 20 and 50 and heat treated at 600°C for 5min

SEM observations show that the addition of water has no effect on the morphology with DEG (agglomerated platelets) and EG (agglomerated spherical particles) (figure 10). However, we can see that for values of $h \geq 2$, the particles are more agglomerated. Such an increase in agglomeration was also observed previously, for the synthesis of ZnO, with an increase in the hydrolysis rate [18]. It could be due to an increase of hydrolysis and condensation kinetics which lead to more dense particles.

DEG 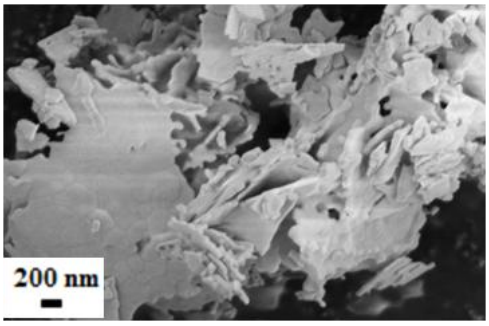

EG 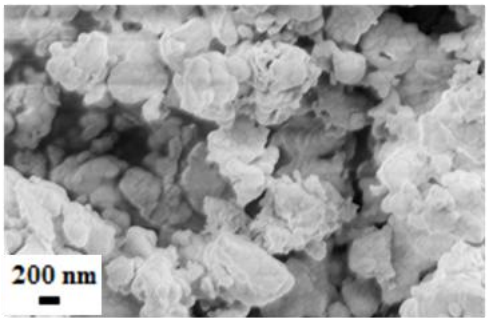

Figure 10: SEM images of the precipitate synthesized with DEG or EG (u = 3) and hydrolysis ratio h = 2, then heat treated at 600°C for 5min.

The addition of water results in a decrease of the specific surface area, as with both EG (4 and 1 $m^2.g^{-1}$ for h equal 2 and 10 respectively) and DEG (8 $m^2.g^{-1}$ for h = 2). The decrease of the specific surface area with EG, despite a decrease in crystallite size, shows that the particles are agglomerated and made of several crystallites.

3.1.4. Effect of the concentration of metal

In the literature, the concentration of dissolved salts is used to control the particle size, the size of particles increasing with concentration [19]. Therefore, we varied the metal concentration [La + Mo] from 0.05 to 0.5 mol L^{-1} (table 4). The different concentrations were tested with DEG (u=0) and EG (u = 3), no water being added. The refluxing time was fixed to 3 hours. The precipitates were heat treated for 5 min at 600 °C.

Table 4: Precipitates synthesized with different concentrations of metal [La + Mb] with DEG or EG and heat treated for 5 min at 600 °C.

Solvent	[La + Mo](mol .L^{-1})	*u*= [urea]/[La+Mo]	Size(nm)	S_{BET} ($m^2.g^{-1}$)
DEG	0.05	0	21	24
DEG	0.1	0	42	11
DEG	0.2	0	41	16
DEG	0.3	0	44	12
DEG	0.4	0	48	7
DEG	0.5	0	43	16
EG	0.05	3	29	6
EG	0.1	3	46	3
EG	0.2	3	50	6
EG	0.3	3	53	5
EG	0.4	3	53	3
EG	0.5	3	57	5

All the powders synthesized with DEG or EG, after a heat treatment at 600°C for 5 min are identified to be pure $La_2Mo_2O_9$ by XRD. The crystallite size was estimated, from XRD patterns (figure 11 and 12), according to the Scherrer equation. From the thinnest diffraction peak at about 2θ=24.9 °, the crystallite size is between 21-48nm with DEG and 29-57nm with EG.

Particles synthesized with concentration of 0.05mol.L^{-1} have the smallest average size, as observed directly on XRD diagrams, but for other concentrations, larger average size remains constant. A synthesis with concentration of metal [La+Mo] of 0.025 mol. L^{-1} in DEG was carried out to see if it is possible to reduce the particle size. However, it was impossible to separate particles even by increasing speed centrifugation at 14,000 rpm^{-1}. This is probably due to the very fine particle size or even to a too low concentration, which is then below the critical concentration for nucleus formation or insufficient for their growth [20].

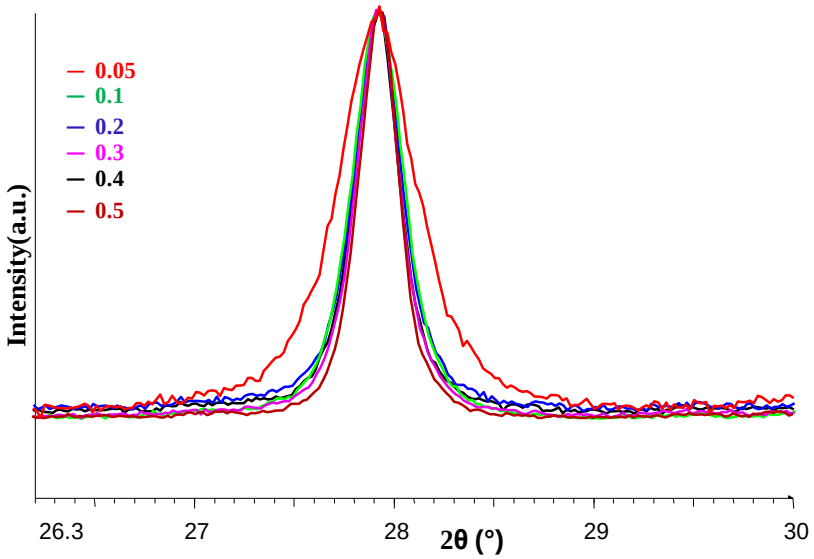

Figure 11: XRD diagrams of precipitates synthesized with DEG, with metal concentrations of 0.05, 0.1, 0.2, 0.3, 0.4 or 0.5 mol.L^{-1} (u = 0) and heat treated at 600°C for 5min

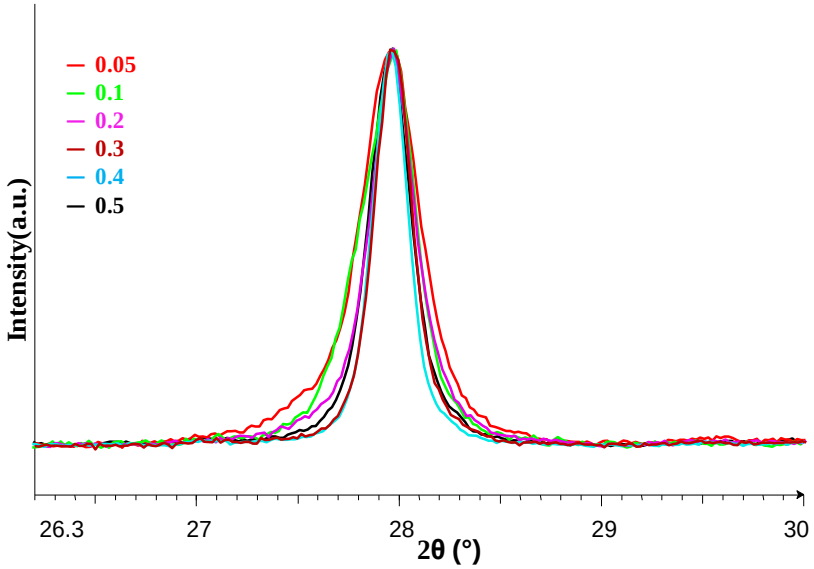

Figure 12: XRD diagrams of precipitates synthesized with EG, with metal concentrations of 0.05, 0.1, 0.2,0.3,0.4 or 0.5 mol.L^{-1} (u = 3) and heat treated at 600°C for 5min.

Whatever the [La + Mo] concentration, SEM observations show generally similar morphologies as platelets or agglomerates of spherical particles, with DEG and EG, respectively (figure 13). However, as shown by XRD, elementary particles (platelets or spheres) have slightly smaller sizes with a [La + Mo] concentration of 0.05 mol.L^{-1}. With this low concentration, the agglomeration of powders also seems less important in the case of DEG; platelets are more likely to organize themselves to form desert roses.

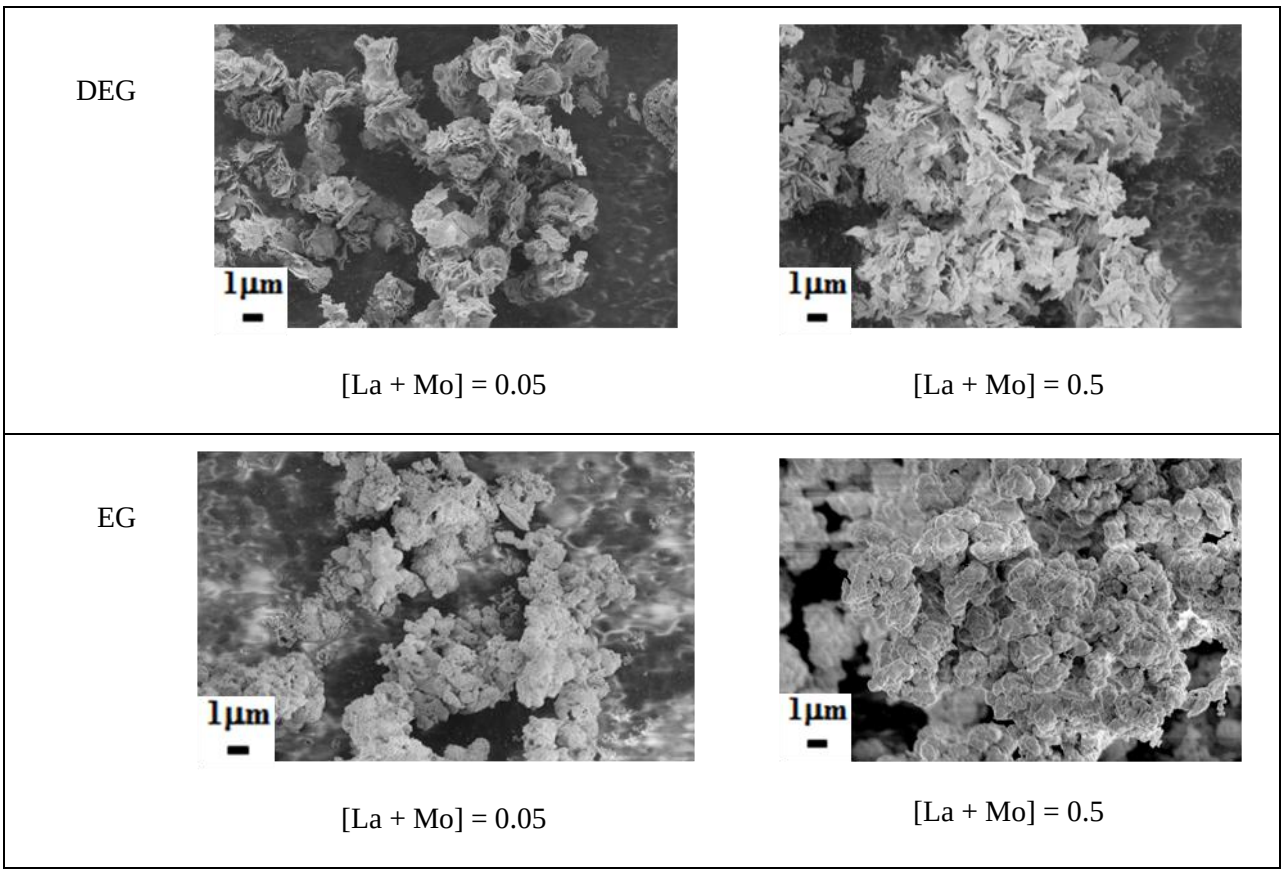

Figure 13: SEM images of precipitates synthesized with metal concentrations [La + Mo] of 0.05 and 0.5 mol.L^{-1} with DEG (u = 0) and EG (u = 3), then heat treated for 5 min at 600 °C.

When the concentration is lowered to [La + Mo] = 0.05 mol.L^{-1}, the crystallite sizes and the agglomerates formed are smaller. This suggests that the decrease in concentration [La + Mo] below a value of 0.1 mol.L^{-1} leads to a decrease in size of the particles formed, as well as their agglomeration.

We measured the specific surface area according to the BET method for all the powders heat treated at 600 °C for 5min (table 4). As expected, in the case of DEG, its evolution is inverse of that of the crystallite size. Indeed, platelets formed by crystallites with smaller sizes have the highest specific surface area. Thus, the surface area of the powder synthesized with a metal concentration [La + Mo] = 0.05 mol.L^{-1} is 24 $m^2.g^{-1}$ when the crystallite size is 21 nm. For higher [La + Mo] concentrations, the specific surface is lower (between 7 and 16 $m^2.g^{-1}$), with a crystallite size of about 40 nm. When EG is used as a solvent, the surface area remains substantially the same (between 3 and 6 $m^2.g^{-1}$), although the crystallite size is significantly smaller than the others (30 nm instead of about 50 nm) with a [La + Mo] concentration of 0.05 mol.L^{-1}. Lowering the [La + Mo] concentration to 0.05 mol.L^{-1} therefore allowed us to obtain, using DEG as solvent, the largest surface area using the conventional polyol method and heat treating the precipitate 5 min at 600 °C.

3.2. Conduction properties

In order to measure the ionic conductivity of our samples and thus estimate the impact of the microstructure, with optimal conditions, it was necessary to determine the sintering parameters that allow to increase the density (in order to decrease grain boundary contribution) while maintaining the grain size as small as possible. The determination of the sintering conditions of powders is thus described before presenting the conductivity properties.

3.2.1. Sinterability and pellets microstructure

In order to estimate the more suitable sintering conditions, we studied the sinterability of the powders. It was first investigated by dilatometry on pellets made of powders obtained by polyol process after a heat treatment at 600 °C for 5 min of the precipitates obtained with DEG (h and u = 0) and EG (h = 0, u = 3), these powders being constituted respectively of platelets and agglomerated spheres. Comparison was made with the sinterability of powder synthesized by conventional solid state reaction (SSR). The powders were compacted in the shape of pellets of 5 mm diameter, by uniaxial pressing under 5000 bar and then isostatic pressing also under 5000 bar. The linear shrinkage of these three samples, under air, from room temperature up to 950 °C with a speed of 5 °C.min^{-1} is presented in figure 14. Comparison of curves evidences a difference of behavior between the two powders synthesized by polyol process.

For the powder obtained with DEG as solvent, a significant linear shrinkage of about 13% is observed beyond 550 °C. This shrinkage is related to the removal of much of the porosity initially present in the pellets. Two mechanisms of shrinkage seem to proceed, as a slight change of the slope can be observed around 650 °C (figure 14). This could be due to a preferential welding of platelets stuck together, in the first step. For the powders obtained with EG, a significant linear shrinkage, of about 11%, proceeds above 620 °C. In this case, two very different regimes of sintering are observable, with an important lowering of the speed about 720 °C. This is probably due to a differential sintering. First, agglomerates, which consist in spherical particles, sinter. This leads to large grains with a large porosity between them. In the second step, the porosity inter-agglomerate decreases with time but far more slowly, leading to a lower densification.

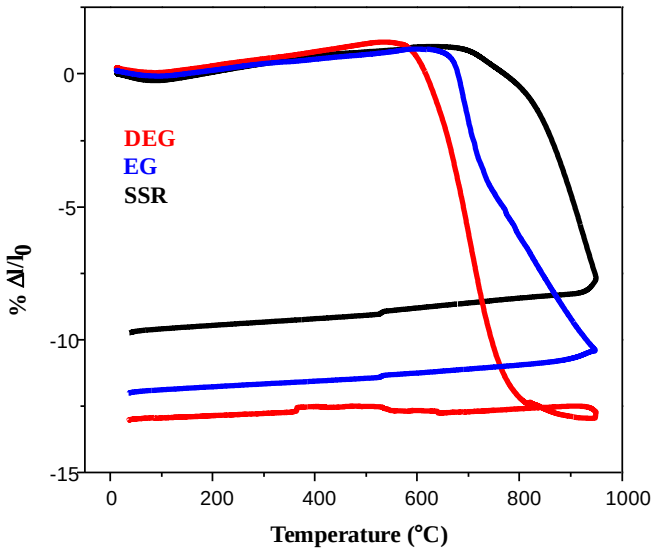

Figure 14: Linear shrinkage as a function of temperature, with a heating and cooling rate of 5°C.min^{-1}, under air, of powders synthesized with DEG (u = 0) or EG (u = 3) and a heat treatment at 600 °C for 5 min, and by solid state reaction (SSR).

According to these results, short sintering times and sintering temperatures of 650 and 750 °C, for the pellets prepared with powders obtained with DEG or EG, respectively, were chosen. Additionally, the pellets were directly placed in a muffle furnace preheated at the desired temperature and, after a heat treatment of 30 min, quenched at room temperature, such a sintering being qualified as rapid sintering in this paper. These conditions seem to be the more appropriate to avoid an important grain growth while obtaining a density as satisfactory as possible for ionic conductivity measurements. In order to favor the electric measurements by increasing the density, rapid heat treatments at 925°C were also done.

The microstructures of the pellets obtained with such rapid heat treatments are then presented.

- Pellets made of powders obtained with DEG (platelets).

Pellets made of the powders obtained with DEG were densified by a rapid sintering at 650 or 925 °C for 30 min, under air. The relative densities reached are of 79 and 95% respectively. A high relative density is thus obtained with these powders after a rapid sintering at 925 °C, the porosity being then closed.

SEM images of pellets sintered at 650 or 925°C and then fractured are presented in figure 15. They evidence the transition from open to closed porosity when increasing the sintering temperature from 650°C (figure 15 a) to 925°C (figure 15 b) as well as the increase in density. For pellet sintered at 650 °C, we can observe the presence of relatively large, interconnected pores (few hundred nanometers) located at grain boundaries, the grain size being in the order of microns. For pellet

sintered at 925°C, the porosity is greatly decreased and closed. Therefore, its relative density is very high.

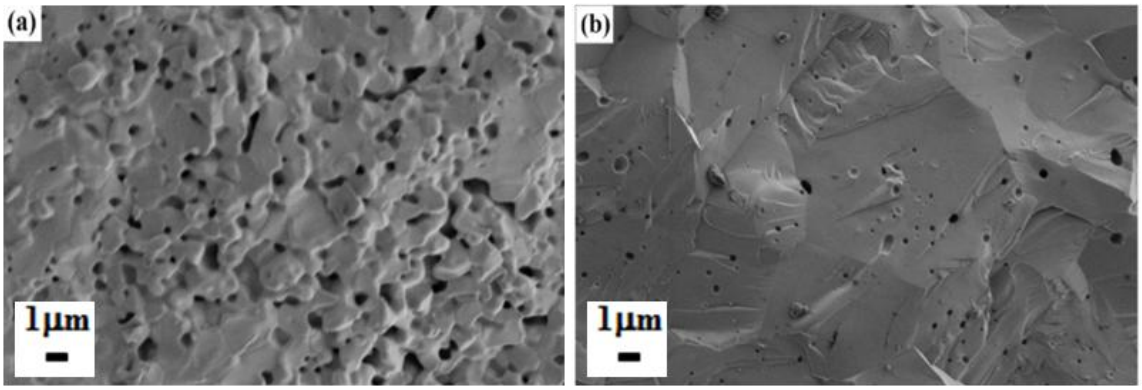

Figure 15: SEM images of pellets, made of a powder obtained after heat treatment for 5 min at 600 °C of the precipitate synthesized in DEG, then sintered at a) 650 °C and b) 925 °C for 30 min.

- Pellets made of powders obtained with EG (spheres).

Pellets made of powders obtained after heat treatment at 600 °C for 5 min of the precipitate synthesized with EG were densified by a quick sintering at 750 or 925 °C for 30 min, under air. Their relative densities are of 78 and 82% respectively. The relative density increases with the sintering temperature, but is still substantially lower than the one reached with the powders prepared with DEG, with a sintering temperature of 925°C. This is in agreement with the dilatometric curves which highlight a lower sinterability of the powders obtained with EG.

SEM images of the pellets sintered at 750 or 925°C for 30 min and then fractured are presented in figure 16. The slight decrease of the relative porosity of pellets with increasing sintering temperature is evidenced. The porosity is highly connected after a sintering at 750 °C and still remains connected after a sintering at 925 °C, even if the grains are more weld together. The size of the grains, that are relatively spherical, remains slightly the same and is in the order of few hundred nanometers.

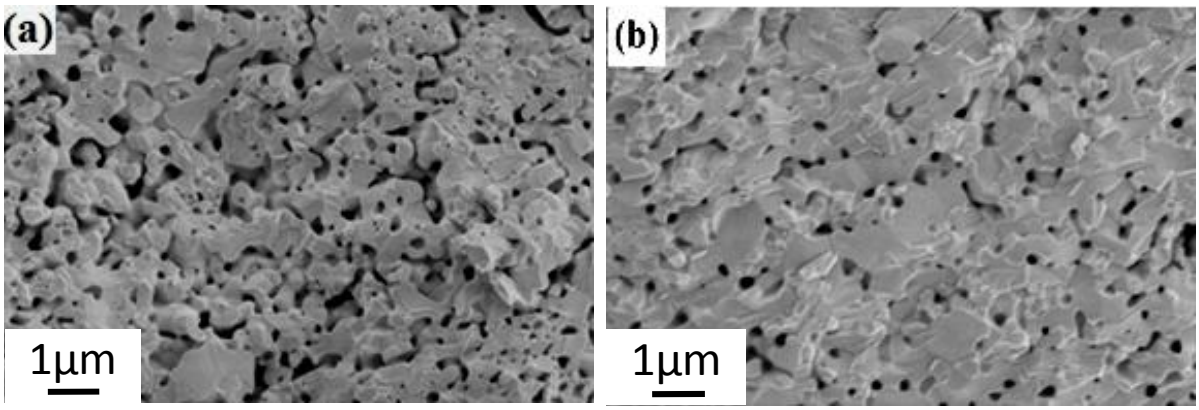

Figure 16: SEM images of pellets, made of a powder synthesized with EG and heat treated at 600 °C for 5 min, then sintered at a) 750 °C and b) 925 °C for 30 min.

- Pellets made of powders obtained by solid state reaction.

In order to determine the impact of the powder synthesis process, a reference pellet was prepared with a powder synthesized by solid state reaction [2]. As evidenced by dilatometry (figure 14), the sinterability of these powders is significantly lower than that of the powders obtained by the polyol process. It was thus necessary to treat these powders by high energy ball milling to increase the relative density as it strongly influences the conductivity [3]. This step allowed to reach a relative density of 98% after a rapid sintering at 925°C. As in the case of pellets made of powders prepared by the polyol process, the relative density of the pellets made from powder synthesized by solid state reaction is higher after a rapid sintering at 925°C than after dilatometry, the relative density being in the last case of 94%. This may be due to the fact that rapid sintering allows to reduce grain growth during the increase in temperature before reaching the sintering temperature.

- Conclusion on sintering of the powders

In conclusion, according to the dilatometric study and the microstructural characterization, a strong difference is observed between the sinterings of spherical particles (obtained with EG) and of platelets (obtained with DEG). Indeed, after a rapid sintering at 925°C, the relative density is markedly higher for the pellets made of platelets, the closure of the porosity being even reached. The lower relative density of the pellets made of spherical particles may be due to a strong agglomeration of the particles that lead to a differential sintering. However, it has to be pointed out that a relative density of about 80%, reached after a rapid sintering at 650 or 750°C for the platelets or spherical particles respectively, is already satisfactory to realize conductivity measurements by impedance spectroscopy in suitable conditions when the grain growth has to be limited as much as possible.

Moreover, it has to be noted that, when sintered pellets are prepared from the powders obtained by the polyol process, a very high relative density (95%) can be reached, without any milling step that would lead to the introduction of impurities, contrarily to the powders obtained by solid state reaction. This is thus an important advantage offered by the powders prepared by the polyol process with DEG, that can be very useful in many applications.

3.2.2. Conductivity measurements

Our aim was to determinate if the grain size and the morphology of the starting powders impact the ionic conduction properties of the $La_2Mo_2O_9$ compound. This part of the work is thus dedicated to the determination of the transport properties of the pellets made of pure $La_2Mo_2O_9$ powders prepared by the polyol process with DEG and sintered at 650 or 925°C or with EG and sintered at 750 or 925°C. The results are compared with those of a reference pellet made of powder prepared by the solid state reaction. The relative densities of the different pellets are of 79, 95, 78, 82 and 98% respectively.

The data were collected in the temperature range 302 - 700°C. The impedance diagram acquired at 327, 352 and 377 °C are presented in figure 17 for the pellets made of powders prepared by polyol process with DEG (u=0) and sintered at 650 (a) or 925 °C (b), and with EG (u = 3) and sintered at 750 (c) or 925 °C (d), and of powder prepared by solid state reaction and sintered at 925°C (e).

The resistance of all the samples decreases with increasing temperature. Up to three contributions can be distinguished. The first contribution (at high frequencies), that is represented as a semicircle and modeled by a parallel circuit R-CPE, can be assigned to the grain contribution. The phenomena observed at intermediate frequencies, called as grain boundaries contributions, correspond to all the phenomena that happen at the grain interfaces. At low frequency, the electrode polarization is observed in some cases, in the form of a straight line or sometimes of an arc of circle. The presence of several relaxations, which can be assigned to the grain and grain boundaries contributions, was already observed for the $La_2Mo_2O_9$ compound synthesized by freeze-drying [22-23] or spray pyrolysis [24]. In the case of the $La_2Mo_2O_9$ powders obtained by solid state reaction and then ball milled and sintering at 925°C, the grain boundaries contribution is very low and cannot generally be distinguished from grain contribution. It is the same for our reference pellet (figure 17 e)).

A significant difference is observed in the case of the pellet made of powder synthesized in DEG and sintered at 650 °C (figure 17 a)). Indeed, the contribution of the grain is characterized by a far lower resistance and therefore a significantly greater conductivity than for the other pellets. However, despite the high conductivity of the grain, the resistance at grain interfaces is very important, leading to a lower total conductivity ($\sigma = 6.8\ 10^{-7}$ S.cm^{-1}) than for other pellets made of powders synthesized by polyol process (σ closed to $2\ 10^{-6}$ S.cm^{-1}) at 377 °C, despite a higher compactness than for the pellets made of powders obtained with EG.

We also observed, for all the pellets, a decrease of the resistance of grains and grain boundaries and a shift of the characteristic frequencies to the high frequencies with increasing temperature, until the second semicircle relative to the grain boundaries contribution completely disappears at higher temperature.

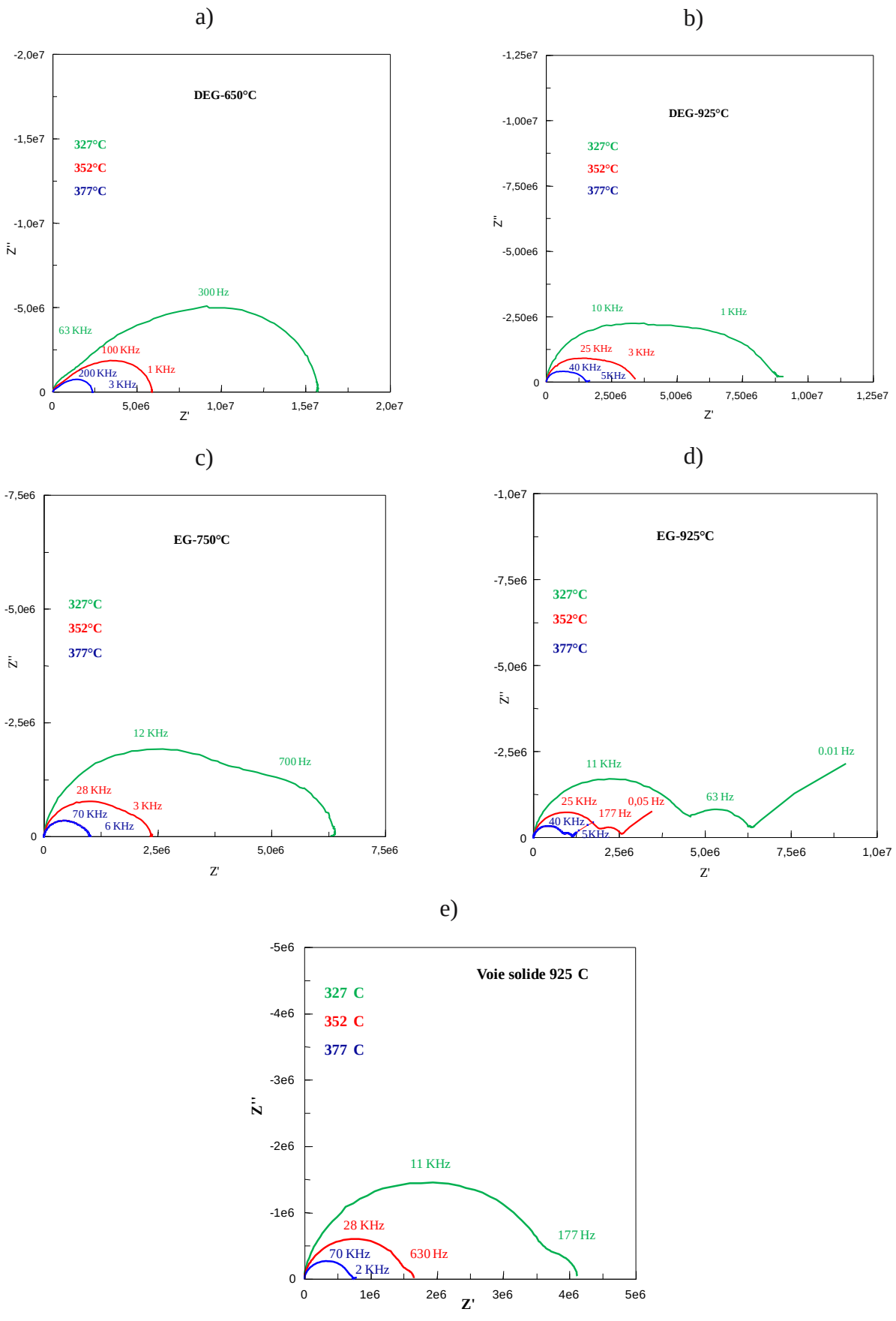

Figure 17: Complex impedance diagram recorded at 327, 352 and 377 °C for pellets made of powders synthesized with DEG and sintered at 650 (a) or 925 °C (b), and with EG (u = 3) and

sintered at 750 (c) or 925 °C (d), and of the powder synthesized by solid state reaction and sintered at 925°C (e).

The modeling of diagram (Z-view software) was thus realized by using several theoretical models that accounted for the evolution of the aspect of the diagram according to the temperature and the sample. Refinements were realized by modeling either with two parallel equivalent circuits R-CPE for the grain and grain boundaries contribution and a CPE for the polarization at electrodes, or with only one parallel equivalent circuit R-CPE (and a CPE) when there is an overlapping of the grain and grain boundaries contributions. In the last case, this is thus the total resistance and conductivity which are determined globally. At high temperature, for all the pellets, no more semicircle corresponding to the migration phenomena is observable and positive values of the imaginary part are even measured. The resistance of the material is then assimilated to the abscissa of the first point for which Z" becomes negative.

The values of the grain, grain boundaries and total conductivities are listed in table 5. For the powder synthesized with DEG and sintered at 650 °C, the grain conductivity is slightly higher but the grain boundaries conductivity is lower, resulting in a total conductivity slightly lower than that of the others pellets. For the same powder but sintered at 925 °C, the ratio between the conductivities of the grains and grain boundaries, σ_g / σ_{gb} at 327 °C is significantly lower (1.6 instead of 16.4) and the total conductivity is very closed to that measured in the case of the powder synthesized with EG and sintered at 925 °C. However, the ratio σ_g / σ_{gb} remains higher than in the case of the powders obtained with EG, for which it is of 0.6 and 0.5 respectively after sintering at 750 or 925 °C.

The expected decrease of the contribution of the grain boundaries, with the increase of the sintering temperature, has also been observed for powders of $La_2Mo_2O_9$ synthesized by freeze drying [23].

Table 5 : Grains (σ_g), grain boundaries (σ_{gb}) and total (σ_t) conductivities at 327, 352 and 377°C, determined by using the software ZView, of pellets made from powders synthesized with DEG and sintered at 650 or 925 °C or with EG (u = 3) and sintered at 750 or 925 °C or of a pellet made from the powder obtained by solid state reaction and sintered at 925°C.

Synthesis method	**Sintering temperature (◦C)**	**Relative density (%)**	**T (°C)**	**σ_g (S.cm^{-1})**	**σ_{gb} (S.cm^{-1})**	**σ_t (S.cm^{-1})**
polyol DEG	650	79	327	$1.8\ 10^{-6}$	$1.1\ 10^{-7}$	$1.0\ 10^{-7}$
			352	$3.8\ 10^{-6}$	$3.0\ 10^{-7}$	$2.8\ 10^{-7}$
			377	$9.3\ 10^{-6}$	$7.3\ 10^{-7}$	$6.8\ 10^{-7}$
	925	95	327	$6.8\ 10^{-7}$	$4.2\ 10^{-7}$	$2.6\ 10^{-7}$
			352	$1.7\ 10^{-6}$	$1.1\ 10^{-6}$	$6.6\ 10^{-7}$
			377	$4.3\ 10^{-6}$	$2.2\ 10^{-6}$	$1.5\ 10^{-6}$
polyol EG	750	78	327	$4.2\ 10^{-7}$	$6.8\ 10^{-7}$	$2.6\ 10^{-7}$
			352	$1.1\ 10^{-6}$	$2.0\ 10^{-6}$	$7.0\ 10^{-7}$
			377	$2.8\ 10^{-6}$	$4.1\ 10^{-6}$	$1.7\ 10^{-6}$
	925	82	327	$4.8\ 10^{-7}$	$9.7\ 10^{-7}$	$3.2\ 10^{-7}$
			352	$1.1\ 10^{-6}$	$2.8\ 10^{-6}$	$8.0\ 10^{-7}$
			377	$2.4\ 10^{-6}$	$6.7\ 10^{-6}$	$1.8\ 10^{-6}$
solid	925	98	327	$4.9\ 10^{-7}$	$4.3\ 10^{-6}$	$4.4\ 10^{-7}$
			352	$1.2\ 10^{-6}$	$1.4\ 10^{-5}$	$1.1\ 10^{-6}$
			377	$2.7\ 10^{-6}$	$3.9\ 10^{-5}$	$2.5\ 10^{-6}$

The Arrhenius plots ($\log(\sigma T) = f(\frac{1000}{T})$) of all the samples are reported in figure 18. For all curves, an abrupt break is observed around of 600 °C. This abrupt change in the anionic conductivity is due to the first order phase transition α / β, the β-form presenting the higher conductivity. On both sides of this break, Arrhenius law is followed. It is interesting to note that the jump in conduction occurs at a slightly lower temperature (between 25 and 50 °C lower) in the case of the pellet made of the powder synthesized with DEG and sintered at 650 °C. Its total conductivity, is always the lowest, except at 602 °C. It can be also observed that the jump in conductivity seems to be less important in the case of powders sintered at 650 °C (prepared from DEG) or 750 °C (prepared with EG). As sintering of the powders was carried out at temperatures as low as possible and for relatively short times (30 min) in order to limit grain growth, the densification of the pellets still proceed at high measurement temperatures. The relative density increased from 79% to 93% and from 78% to 81% for pellets made of the powders synthesized with DEG and EG respectively. However, the evolution of the sample dimensions does not affect significantly the shape factors and the conductivities that are deduced from it. For example, at 702 °C, total conductivities calculated with the new shape factor, are only slightly higher ($5.98\ 10^{-3}$ instead of $5.58\ 10^{-3}$ S.cm^{-1} or $7.57\ 10^{-3}$ instead of $7.45\ 10^{-3}$ S.cm^{-1} with respectively DEG or EG). Nevertheless, for the pellet made of the powder synthesized with EG and sintered at 750 °C, the carrying out of sintering during the measurements (at the highest temperatures), can explain the

slight breaking of the conductivity beyond 652 °C. In the case of the pellet made of the powder synthesized with DEG and sintered at 650 °C, we probably do not observe this small breaking of the conductivity as the sintering temperature of the powder is lower (beginning between 550 and 600 °C) and coincides with the one of the α↔β phase transition, this transition leading to an increase of the conductivity.

It can be noted that, except at 602 °C, the conductivity of the pellet made of the powder synthesized by solid state reaction is always slightly higher than the ones of the pellets made of the powders synthesized by the polyol process. This can be explained by the amount of grain boundaries which is lower in the samples prepared from powders synthesized by solid state reaction. In this case, the total conductivity is quite not affected by the grain boundaries resistance as their contribution is weaker.

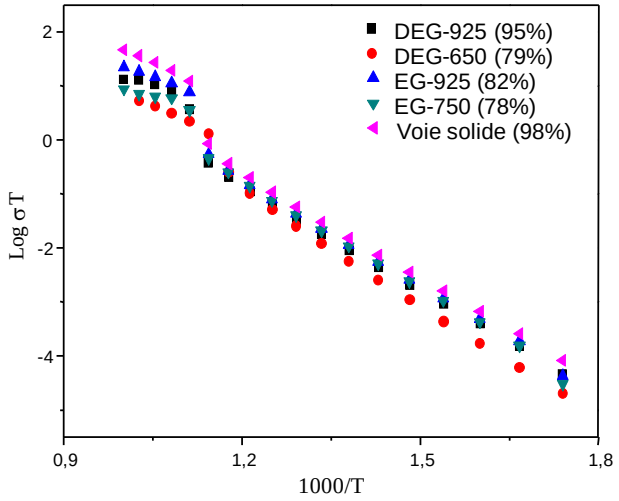

Figure 18 : Arrhenius plot of the ionic conductivity of the pellets made of powders synthesized with DEG and sintered at 650 °C or 925 °C or with EG (u = 3) and sintered at 750 or 925 °C or prepared by solid state reaction and sintered at 925 °C.

The activation energies, estimated from the slope of the segments between 300 and 600 °C and between 625 °C and 725 °C of the Arrhenius plot, are presented in table 6. All the samples present very similar activation energies, around 1.3 eV, for the first segment. However, this value is slightly higher in the case of the pellet made of the powder synthesized with DEG and sintered at 650 °C. For the second segment, the value of the activation energy is lower, between 0.61 and 1.03 eV. However, this variation is not really representative, as some shape factors evolved during measurements at the highest temperatures (above 600 °C).

Table 6 : Activation energies between 300 and 600 °C and between 625 and 725 °C for the pellets made of powders synthesized with DEG and sintered at 650 or 925 °C or with EG (u = 3) and sintered at 750 or 925 °C or synthesized by solid state reaction (SSR) and sintered at 925 °C.

Synthesis method	Sintering temperature (◦C)	Ea (eV) between 300°C and 600°C	Ea (eV) between 625°C and 725°C
SSR	925	1.26	1.01
DEG	650	1.42	1.03
DEG	925	1.27	0.73
EG	750	1.33	0.61
EG	925	1.31	0.81

According to all these results, we can establish that the evolution of the conductivity of the samples synthesized by polyol process is similar to that of the samples synthesized by solid state reaction. However, the values are slightly lower. This can be attributed to the high amount of grain boundaries that create an effect of "blocking" in our case, leading to their higher contribution in the resistance to ion migration. Therefore, the measured total conductivity is lower than that determined when the initial powder is synthesized by solid state reaction as the ratio of grain boundaries is very low in this case.

The same behavior was observed for the $La_2Mo_2O_9$ compound synthesized by freeze drying and sintered at temperatures lowers than 925°C, the relative density being less than 92% [23]. As in many cases, it is difficult to completely benefit of conduction properties probably improved by nanometric particles.

4. Conclusion

Nanostructured $La_2Mo_2O_9$ powders were synthesized by the polyol process, with two different morphologies (platelets or spheres) according to the nature of the solvent. Obtaining crystallized nanodomains can be achieved by the polyol process as it presents the advantage of a relatively low temperature thermal treatment (around 550-600°C). In order to determine the effect of the main synthesis parameters on the powder microstructure and purity, we varied also the refluxing time, the hydrolysis ratio, the metal concentration and we had hydroxide ions by the means of urea.

The ionic conduction properties were determined. First of all, the sinterability of the powders was evaluated in order to determine the more appropriate sintering temperature that allows obtaining relatively dense pellets while preserving as much as possible the grain size. It was established that the powders synthesized with DEG as solvent present a very high sinterability, relative densities of 95% being reached without any intermediate step as milling, contrarily to the solid state reaction for

example. The values of the ionic conductivity are close to the ones of the powders synthesized by solid state reaction but always lower, except at 602°C, for the powder synthesized with DEG and rapidly sintered at 600°C. The lower values of the total conductivity can be explained by the high amount of grain boundaries in the pellets made from the powders synthesized by the polyol process. In our case, they lead to a contribution of grain boundaries to the total resistance of the pellets that can be very important. However, despite slightly lower conduction properties, the efficient sintering of such nanoparticles, with no milling step could be of great interest for further applications (better long term stability and performances of the material).

Acknowledgements

We would like to acknowledge the Ministère de l'Enseignement Supérieur et de la Recherche Scientifique of the Tunisian Republic and the Ecole Doctorale Matière, Molécules et Matériaux en Pays de la Loire (3MPL)(ED500) for their financial support. The authors also express their thanks to Melanie Joly and Cyrille Bruneau, from the IUT of Le Mans, for their help with BET measurements.

References

1. P. Lacorre, F.Goutenoire, O.Bohnke, R.Retoux, Y.Laligant, Designing fast oxide-ion conductors based on $La_2Mo_2O_9$, Nature 404 (2000) 856-858.

2. F. Goutenoire, O.Isnard, R.Retoux, P.Lacorre, Crystal structure of $La_2Mo_2O_9$, a new fast oxide-ion conductor, Chemical Materials12 (2000) 2575-2580.

3. S. Georges, F. Goutenoire, F. Altorfer, D. Sheptyakov, F. Fauth, E. Suard, P. Thermal, Structural and transport properties of the fast oxide-ion conductors $La_{2-x}R_xMo_2O_9$ (R=Nd, Gd, Y), Solid State Ionics 161 [3-4] (2003) 231-241.

4. J. Yang, Z. Gu, Z. Wen, D. Yan, Preparation and characterization of solid electrolytes $La_{2-x}A_xMo_{2-y}W_yO_9$ (A=Sm, Bi), Solid State Ionics 176 [5-6] (2005) 523-530.

5. J. E. Vega-Castillo, U. K. Ravella, G Corbel, P. Lacorre, A. Caneiro, Thermodynamic stability, structural and electrical characterization of mixed ionic and electronic conductor $La_2Mo_2O_{8.96}$, Dalton trans. 41 (2012) 7266-7271.

6. F. Goutenoire, O. Isnard, E. Suard, O. Bohnke, Y. Laligant, R. Retoux, P. Lacorre, Structural and transport characteristics of the LAMOX family of fast oxide-ion conductors, based on lanthanum molybdenum oxide $La_2Mo_2O_9$, J. Mater. Chem. 11 (2001) 119–124.

7. S. Georges, F. Goutenoire, P. Lacorre, M.C. Steil, Sintering and electrical conductivity in fast oxide ion conductors $La_{2-x}R_xMo_{2-y}W_yO_9$ (R: Nd, Gd, Y), J. Eur. Ceram. Soc. 25 [16], (2005) 3619-3627.

8. S. Georges, S. Skinner, P. Lacorre, M.C. Steil, Oxide ion diffusion in optimised LAMOX materials, Dalton Trans. 19 (2004) 3101-3105.

9. C.N. Rao, S. Gopalakrishnan, New directions in solid state chemistry, Cambridge University Press, Cambridge, 1986.

10. H. Sellemi, S. Coste, A. Ben Ali, R. Retoux, L.S. Smiri, P. Lacorre, Synthesis of $La_2Mo_2O_9$ powders with nanodomains using polyol procedure, Ceram. Int. 39 [8] (2013) 8853-8859.

11. D. Larcher, G. Sudant, R. Patrice, and J.-M. Tarascon, Some insights on the use of polyols-based metal alkoxides powders as precursors for tailored metal-oxides particles, Chem. Mater. 15 (2003) 3543–3551.

12. S. D. Škapin, I. Sondi, Synthesis and characterization of calcite and aragonite in polyol liquids: control over structure and morphology, J. Colloid Interf. Sci. 347 (2010) 221–226.

13. R. Justin Joseyphus, B. Jeyadevan, Low temperature synthesis of ITO nanoparticles using polyol process, J.Phys. Chem. Solids 72 (2011) 1212–1217.

14. M.A. Flores-Gonzalez, G. Ledoux, S. Roux, K. Lebbou, P. Perriat, O. Tillement, Preparing nanometer scaled Tb-doped Y_2O_3 luminescent powders by the polyol method, J. Solid State Chem. 178 [4] (2005) 989-997.

15. M. Barré, F. Le Berre, M-P. Crosnier-Lopez, C. Galven, O. Bohnké, J-L. Fourquet, The NASICON solid solution $Li_{1-x}La_{x/3}Zr_2(PO_4)_3$: optimization of the sintering process and ionic conductivity measurements, Ionics 15 (2009) 681-687.

16. D. Johnson Zview Software, 3.0a; Scribner Associates, Inc: 2005

17. W. Kuang, Y.Fan, Yao, K. Chen, Y., Synthesis, characterization and optical properties of ZnO nanoparticles with controlled size and morphology, J. Solid State Chem. 140 [2] (1998) 354-360.

18. A. Dakhlaoui, M. Jendoubi, L.S. Smiri, A. Kanaev, N. Jouini, Synthesis, characterization and optical properties of ZnO nanoparticles with controlled size and morphology, J. Cryst. Growth 311 [16] (2009) 3989-3996.

19. L.Poul, N. Jouini, F. Fiévet, Layered Hydroxide Metal Acetates (Metal = Zinc, Cobalt, and Nickel): Elaboration via Hydrolysis in Polyol Medium and Comparative Study, Chem. Mater. 12 [10] (2000) 3123-3132.

20- C.J. Brinker et G.W. Scherer, Sol-Gel Science: The Physics and Chemistry of Sol-Gel Processing, Academic Press, New York (1990).

21. E. Hammarberg, A. Prodi-Schwab, C. Feldmann, Microwave-assisted polyol synthesis of aluminium- and indium-doped ZnO nanocrystals, J. Colloid Interf Sci. 334 [1] (2009) 29-36.

22. D.Marrero-Lopez, J. C.Ruiz-Morales, P. Nunez, J. C. C.Abrantes, J. R. Frade, Synthesis and characterization of $La_2Mo_2O_9$ obtained from freeze-dried precursors, J. Solid State Chem. 177 [7] (2004) 2378-2386.

23. D.Marrero-López, J. Canales-Vázquez, J. C. Ruiz-Morales, A. Rodríguez, J. T. S. Irvine, P. Núñez, Synthesis, sinterability and ionic conductivity of nanocrystalline $La_2Mo_2O_9$ powders, Solid State Ionics 176 [23-24] (2005) 1807-1816.

24. L.Baqué, J. Vega-Castillo, S. Georges, A. Caneiro, E. Djurado, Microstructural and electrical characterizations of tungsten-doped $La_2Mo_2O_9$ prepared by spray pyrolysis, Ionics 19 [12] (2013) 1761-1774.

Figure captions

Figure 1: XRD diagrams of precipitates synthesized with DEG with a reflux time of 1, 2 or 3 hours and heat treated at 600°C for 5 min.

Figure 2: XRD diagrams of precipitates synthesized with different polyols : EG, PEG and TEG and heat treated at 600°C for 5 min.

Figure 3: XRD diagrams of precipitates synthesized a) with DEG (u = 1, 2 or 3) and b) with EG (u = 2, 3 or 4) and heat treated at 600°C for 5 min.

Figure 4: XRD diagrams of precipitates synthesized with PEG (u = 3) or TEG (u = 3) and heat treated at 600°C for 5min.

Figure 5: SEM images of precipitates synthesized with DEG (u = 3) (a) or with EG (u = 3) (b) and heat treated at 600°C for 5min.

Figure 6: TEM images of the precipitate synthesized with EG (u=3) and heat treated at 600°C for 5min.

Figure 7: SEM images of precipitates synthesized with PEG (u = 3) or TEG (u = 3) and heat treated at 600°C for 5min.

Figure 8: XRD diagrams of the precipitate synthesized with DEG and hydrolysis ratio h equal 0, 2, 10, 20 and 50 and heat treated at 600°C for 5min

Figure 9: XRD diagrams of the precipitate synthesized with EG and hydrolysis ratio h equal 0, 2, 10, 20 and 50 and heat treated at 600°C for 5min

Figure 10: SEM images of the precipitate synthesized with DEG or EG (u = 3) and hydrolysis ratio h = 2, then heat treated at 600°C for 5min.

Figure 11: XRD diagrams of precipitates synthesized with DEG, with metal concentrations of 0.05, 0.1, 0.2, 0.3, 0.4 or 0.5 mol.L^{-1} (u = 0) and heat treated at 600°C for 5min

Figure 12: XRD diagrams of precipitates synthesized with EG, with metal concentrations of 0.05, 0.1, 0.2,0.3,0.4 or 0.5 mol.L^{-1} (u = 3) and heat treated at 600°C for 5min.

Figure 13: SEM images of precipitates synthesized with metal concentrations [La + Mo] of 0.05 and 0.5 mol.L^{-1} with DEG (u = 0) and EG (u = 3), then heat treated for 5 min at 600 °C.

Figure 14 : XRD diagrams of precipitates synthesized with DEG, and DDAB concentrations of 0.5, 1, 2, 3, 4 and 5 mmol.L^{-1} and heat treated at 600°C for 5min.

Figure 15: XRD diagrams of precipitates synthesized with EG, and DDAB concentrations of 0.5, 1, 2, 3, 4 and 5 mmol.L^{-1} and heat treated at 600°C for 5min.

Figure 16: SEM images of precipitates synthesized with concentrations of DDAB of 0.5 mmol.L^{-1} with DEG and 2 or 5 mmol.L^{-1} with EG, then heat treated for 5 min at 600 °C.

Figure 17: TEM image of a) the precipitate synthesized with DEG with a concentration of DDAB of 0.5 mmol.L^{-1} and b) the precipitate synthesized with EG with a concentration of DDAB of 5 mmol.L^{-1}, and heat treated at 600 °C for 5 min.

Figure 18: XRD diagrams of precipitates synthesized with DEG, and PVP concentrations of 2 or 4 mmol.$L^{-1}$and heat treated at 600°C for 5min.

Figure 19: XRD diagrams of the precipitates synthesized with EG, and PVP concentrations of 2 or 4 mmol.$L^{-1}$and heat treated at 600°C for 5min.

Figure 20: Linear shrinkage as a function of temperature, with a heating and cooling rate of 5°C.min^{-1}, under air, of powders synthesized with DEG (u = 0) or EG (u = 3) and a heat treatment at 600 °C for 5 min, and by solid state reaction (SSR).

Figure 21: SEM images of pellets, made of a powder obtained after heat treatment for 5 min at 600 °C of the precipitate synthesized in DEG, then sintered at a) 650 °C and b) 925 °C for 30 min.

Figure 22: SEM images of pellets, made of a powder synthesized with EG and heat treated at 600 °C for 5 min, then sintered at a) 750 °C and b) 925 °C for 30 min.

Figure 23: Complex impedance diagram recorded at 327, 352 and 377 °C for pellets made of powders synthesized with DEG and sintered at 650 (a) or 925 °C (b), and with EG (u = 3) and sintered at 750 (c) or 925 °C (d), and of the powder synthesized by solid state reaction and sintered at 925°C (e).

Figure 24 : Arrhenius plot of the ionic conductivity of the pellets made of powders synthesized with DEG and sintered at 650 °C or 925 °C or with EG (u = 3) and sintered at 750 or 925 °C or prepared by solid state reaction and sintered at 925 °C.